

Chapter II

Characterization of a Reconstituted System to Measure SNARE-Driven Vesicle-Vesicle Docking and Fusion Kinetics

2.1) Summary

We describe a reconstituted system to measure SNARE-driven docking and fusion kinetics. The general design comes from a docking and fusion assay designed by the Ha group (Yoon et al., 2006). Here we perform quantitative modeling to predict the FRET efficiencies of the docked but unfused and docked and fused states. Our modeling suggests that for the vast majority of vesicle pairs the docked but unfused state can be distinguished from the docked and fused state. We establish a FRET efficiency threshold based on the results from the modeling ($E = 0.25$) to distinguish between docked but unfused from docked and fused states.

2.2) Introduction

First Generation Docking and Fusion Assays

The first generation of reconstituted SNARE-driven docking and fusion assays studied free v-SNARE vesicles docking and fusing with t-SNARE bilayers supported on glass. In a system developed in our lab, v-SNARE vesicles docked with nearly diffusion-limited kinetics to a low-density t-SNARE bilayer. Docked vesicles fused with the supported bilayer membrane on a 5-10-ms timescale (Liu et al., 2008; Liu et al., 2005; Wang et al., 2009). The docking and fusion kinetics were very similar in the absence and presence of 1 mM Ca^{2+} . Docking and fusion were insensitive to the presence of SNAP-25 (Liu et al., 2005).

The Chu group also studied v-SNARE vesicles docking and fusing with a low-density t-SNARE bilayer. They found that syb and syx were sufficient to dock vesicles but vesicle fusion was always synchronized with when they turned on their laser. They concluded that vesicle fusion required thermal energy from laser heating (Bowen et al., 2004). Similar to Liu's result, they found that neither docking nor fusion was sensitive to SNAP-25. In a third study, the Simon group reported fusion of docked v-SNARE vesicles to a t-SNARE bilayer triggered Ca^{2+} or Mg^{2+} (Fix et al., 2004).

None of these reconstituted systems reproduce well-known aspects of the physiology of SNARE-driven exocytosis. SNAP-25 has been shown in vitro to be required for the formation of a stable ternary SNARE complex and required for vesicle exocytosis in vivo (Brunger, 2005; Rizo and Sudhof, 2002).

One problem with studying fusion of vesicles to supported lipid bilayers on glass is that there is only a 1-3 nm water-filled space between the bilayer and the glass support (Johnson et al., 1991; Kiessling and Tamm, 2003). This close proximity causes proteins and/or lipids in the supported lipid bilayer to interact strongly with the glass. Bowen and coworkers studied the diffusion of syx in their t-SNARE bilayers using Fluorescence Recovery After Photobleaching (FRAP). They found that only 3-7% of their syx was mobile with an average diffusion coefficient (D) of $0.07 \mu\text{m}^2/\text{s}$ (Bowen et al., 2004).

Recent work in our laboratory studied diffusion of syx and DiD, a fluorescently labeled lipid, in giant unilamellar vesicles (GUVs). GUVs were ruptured into planar bilayer patches onto two different surfaces. When bilayer patches were tethered to a PEG polymer-functionalized lipid bilayer on glass more than 80% of both syx and DiD in the GUV exhibited free, homogeneous diffusion with a diffusion coefficient of $\sim 5.5 \mu\text{m}^2/\text{s}$. When the bilayer patches were formed on bare glass, the diffusion coefficients of both syx and DiD were more than 10 times slower (Wang et al., 2010).

Second Generation Docking and Fusion Assays

Second generation docking and fusion assays have been developed to minimize interactions between the proteins and the lipids under study and the underlying support. The Tamm group developed a novel tethered supported lipid bilayer where the lower leaflet of the bilayer was formed by Langmuir-Blodgett transfer and the upper leaflet by spontaneous proteoliposome fusion. The bottom leaflet of their bilayer is covalently pinned to a glass support via a PEG₇₇ linker. In the presence of the hydrophilic PEG₇₇ polymer the gap between their

planar lipid bilayer is ~ 4 nm. Single particle tracking showed that the majority of the lipids and stabilized t-SNARE complexes in these PEG-cushioned bilayers were laterally mobile with $D = 0.14\text{--}0.68 \mu\text{m}^2/\text{s}$ (Domanska et al., 2009; Wagner and Tamm, 2000). The Tamm group found that v-SNARE vesicles fused rapidly to PEG-cushioned t-SNARE bilayers. Fusion was sensitive to the presence of SNAP-25, but required that the t-SNAREs be purified in the presence of a fragment of syb, syb(49-96) (Domanska et al., 2009; Domanska et al., 2010; Kiessling et al., 2010).

The Rothman group included 5% PEG₂₀₀₀-lipids into t-SNARE vesicles to simulate the crowded environment of the plasma membrane. They used these vesicles to make a planar lipid bilayer that was suspended ~ 4 nm from the surface of the glass due to the inclusion of PEG. FRAP showed that the lipids in that bilayer were highly mobile with $D_{lipid} = 3.4 \pm 5 \mu\text{m}^2/\text{s}$. Free v-SNARE vesicles docked and fused with this tethered bilayer 12-times faster in the presence of the binary t-SNARE complex than in the presence of syx alone (Karatekin et al.).

The Ha group designed the first SNARE-driven single vesicle docking and fusion assay (Yoon et al., 2006). They labeled one set of vesicles with 2% DiI, green-fluorescence FRET donors and the other set of vesicles with 2% DiD, red-fluorescent FRET acceptors. They tethered one set of vesicles to a PEG-functionalized glass support. They used the extent of Förster resonance energy transfer (FRET) from the green labels to the red labels to distinguish docked but unfused t-SNARE/v-SNARE vesicle pairs from docked and fused pairs (Yoon et al., 2006). This assay has been used to study the effects of complexin (Yoon et al., 2008), Munc-18 (Diao et al., 2010), and synaptotagmin1 (Christensen et al., 2011; Diao et al., 2009; Lee et al., 2010) on the SNARE-driven docking and fusion kinetics.

We used same strategy as the Ha group for the basis for our new SNARE-bearing reconstituted system. Instead of tethering the vesicles to a PEG-functionalized glass slide, we tethered the vesicles to a PEG polymer-functionalized lipid bilayer on glass. This surface was developed in collaboration with Tingting Wang in our group, who showed that proteins and lipids present in a bilayer patch exhibited free, homogeneous diffusion when tethered to this surface (Wang et al., 2010). Here we perform quantitative modeling to establish a FRET efficiency threshold to sort docked but unfused vesicles pairs from docked and fused pairs. The modeling takes into account the relative size distributions of the v- and t-SNARE vesicles and the Förster radius of the DiI-DiD FRET pair.

2.3.) Results

Size Distributions of Reconstituted v-SNARE and t-SNARE Vesicles

We immobilized hundreds of DiI-labeled t-SNARE vesicles and DiD-labeled v-SNARE vesicles. Background-corrected integrated intensities were placed on a common scale by accounting for differences in the excitation and detection sensitivities (see Experimental Procedures). Histograms of the relative vesicle radii for the populations of v-SNARE and t-SNARE were obtained by taking the square root of each vesicle's corrected intensity value; these are presented in Fig. 2-1. The common radius scale is relative to the mean t-SNARE vesicle radius, which is set to one. The distributions of v-SNARE and t-SNARE vesicle radii are similar overall. The mean t-SNARE vesicle radius (Fig. 2-1*a*) is ~110% the mean v-SNARE vesicle radius (Fig. 2-1*b*). For both v-SNARE and t-SNARE vesicles, ~90% of the vesicles differ in radius by a factor of two or less.

Model Calculations of FRET Efficiencies for Docked and Fully Fused Vesicle Pairs

Full fusion between a vesicle labeled with 2% donors and a vesicle labeled with 2% acceptors results in a product vesicle whose final concentrations are less than 2% and dependent on the relative surface area of the two vesicles. When two equal-sized vesicles dock and fully fuse together the product vesicle has 1% of each label in each leaflet.

Here we calculate the range of FRET efficiency values expected for a docked and fully fused vesicle pair with each vesicle labeled at 2% with DiI or DiD. Because FRET efficiency

falls off rapidly with distance, we modeled each vesicle lipid bilayer as two infinite parallel planes. Each plane contains a random distribution of donors and acceptors. The model assumes that the positions of the labels do not change, that there is no excitation transfer between donor labels, and that R_0 is the same for all donor-acceptor pairs. When these assumptions are met, the infinite plane model geometry accurately predicts the FRET efficiency of donors present in the same membrane as acceptors in small (~28 nm diameter) lipid vesicles (Fung and Stryer, 1978).

Donors undergo FRET to acceptors with an efficiency E that can be determined using (Fung and Stryer, 1978):

$$E = 1 - \frac{1}{\tau_0} \int_0^{\infty} e^{-t/\tau_0} e^{-\sigma S(t)} dt \quad (1).$$

For our infinite parallel plane geometry, σ is the surface density of acceptor labels in labels/nm², τ_0 is the characteristic fluorescence lifetime of the donor labels in the absence of FRET, and $S(t)$ has two terms, one for each plane containing a random distribution of acceptors. The first term is from acceptors in the same plane as the donors where the distance of closest approach (lower limit of the integral) between the labels is a , the center-to-center distance between labels. The second term represents the parallel plane containing acceptors that is separated by a distance h from the donor plane,

$$S(t) = \int_a^{\infty} \left[1 - e^{-\left(\frac{t}{\tau_0}\right) \left(\frac{R_0}{r}\right)^6} \right] 2\pi r dr + \int_h^{\infty} \left[1 - e^{-\left(\frac{t}{\tau_0}\right) \left(\frac{R_0}{r}\right)^6} \right] 2\pi r dr \quad (2).$$

R_0 is the Förster radius of the FRET pair. To estimate the R_0 of the DiI-DiD FRET pair, we collected an absorption spectrum $\varepsilon_A(\lambda)$ for DiD and a fluorescence emission spectrum $F_D(\lambda)$ for DiI and inserted these into the standard equation (Lakowicz, 2006):

$$R_0^6 = \frac{9000(\ln 10)\kappa^2\phi_D}{128\pi^5 N_A n^4} \int_0^\infty F_D(\lambda)\epsilon_A(\lambda)\lambda^4 d\lambda \quad (3)$$

Here N_A is Avogadro's number, n is the index of refraction, ϕ_D is the donor fluorescence quantum yield, and κ^2 is the orientation factor. We assumed that the donor and acceptor transition dipoles are confined to a common plane, in which case $\kappa^2 = 2$ (Gullapalli et al., 2008). The range of literature values for the DiI fluorescence quantum yield is 0.07-0.21 (Sims et al., 1974; Tsien, 1995), corresponding to $R_0 = 5.4$ – 6.5 nm.

We used Mathcad (Parametric Technology Corporation, Needham, MA) to numerically integrate Eqs. 1 and 2 and calculate E vs the percentage of acceptor labels in the membrane. We assumed that each lipid or label occupies 0.65 nm^2 of surface area ($\sigma = \% \text{ acceptors} \cdot 0.015 \text{ nm}^{-2}$). The value used as the distance of closest approach between labels was our estimate for the average center-to-center distance between lipids ($a = 0.84 \text{ nm}$) and the distance between planes was our estimate for the thickness of a lipid bilayer ($h = 4 \text{ nm}$). The results are presented in Fig. S6 for $R_0 = 5, 6$, and 7 nm .

We experimentally tested these models by reconstituting vesicles with a range of DiI and DiD concentrations. We used three different acceptor concentrations: 0.1%, 0.33%, and 1% DiD with DiI (the donor) at two different concentrations for each acceptor concentration. The specific “high donor” mixtures were: 0.1% DiD + 1.9% DiI, 0.33% DiD + 1.67% DiI, 1% DiD + 1% DiI, and “low donor” mixtures were: 0.1% DiD + 0.48% DiI, 0.33% DiD + 0.42% DiI, and 1% DiD + 0.25% DiI. We measured the FRET efficiencies of hundreds of immobilized vesicles for each of the 6 labeling mixtures (Eq. 16 and Experimental Methods). The mean experimental FRET efficiency values are plotted in Fig. 2-2 vs the percentage of acceptors. The experimental FRET

efficiency values agree reasonably well with our models for $R_0 = 5-7$ nm, which lends support to the calculations. Importantly, the FRET efficiency values at a given acceptor concentration agree to within $\sim 20\%$ when the donor concentrations are varied a factor of four (Fig. 2-2), which argues against significant excitation transfer among donors (homoFRET).

Calculated FRET Efficiencies for Docked but Unfused Vesicle Pairs

Docked but unfused vesicles were modeled as a pair of touching spheres. Each sphere has two surfaces (“lipid bilayer leaflets”) that are separated by 4 nm and decorated with a random distribution of labels. A coordinate for each label was generated by assigning a random azimuthal angle (sampled from a uniform distribution) and a random polar angle (sampled from a cosine distribution) using MATLAB.

We then used the label coordinates to calculate a Förster transfer rate for each donor label. First we calculated a list of distances $r_{D_j-Acc_i}$ between the position of donor j and each of the N_{Acc} acceptor labels. We used these distances to calculate the final transfer rate from that particular donor label to each of the acceptor labels, assuming the rate follows the distance dependence expected from Förster theory. The sum of the parallel rates gives us the transfer rate k_{T,D_j} from each donor (Förster, 1948):

$$k_{T,D_j} = \frac{1}{\tau_0} \sum_{i=1}^{N_{Acc}} \left(\frac{R_0}{r_{D_j-Acc_i}} \right)^6 \quad (4)$$

where R_0 is the Förster radius and τ_0 is the donor’s lifetime in the absence of acceptors. The FRET efficiency of each donor j is calculated from:

$$E_{D_j} = \frac{k_{T,D_j}}{k_{T,D_j} + k_{rad} + k_{nr}} = \frac{\sum_{i=1}^{N_{Acc}} \left(\frac{R_0}{r_{D_j-Acc_i}} \right)^6}{\sum_{i=1}^{N_{Acc}} \left(\frac{R_0}{r_{D_j-Acc_i}} \right)^6 + 1} \quad (5)$$

where $\tau_0 = (k_{rad} + k_{nr})^{-1}$ is the donor fluorescence lifetime in the absence of FRET.

The linear laser polarization and the distribution of orientations of absorption transition dipoles on the donor vesicle surface makes an inhomogeneous distribution of donor excitation efficiency. The experiment uses the lipophilic dye DiI as the donor label. When DiI partitions into a lipid bilayer its absorption transition dipole moment preferentially orients parallel to the bilayer surface (Axelrod, 1979). To estimate the FRET efficiency of docked but unfused pairs excited by linearly polarized light, we must account for preferential excitation of DiI molecules whose transition dipoles lie parallel to the polarization axis. The probability of absorption is proportional to the square of the cosine of the angle between the donor absorption transition dipole and the electric field vector \mathbf{E} (Lakowicz, 2006). Here we estimate the relative excitation efficiency for donor labels of different orientation by making the following simplifying assumptions: the vesicles are spherical, all DiI transition dipoles are aligned parallel to the vesicle surface, the evanescent wave is s-polarized such that \mathbf{E} has only an x-component, and the transition dipoles sample all orientations within the plane of the bilayer uniformly. We also assume that the fluorescence collection efficiency does not depend on the donor orientation, which has been shown to be a reasonable assumption for collection of fluorescence within 500 nm of the glass coverslip using a high numerical aperture objective (Anantharam et al.).

In our models each donor transition dipole moment is located at a position on the vesicle specified by spherical polar coordinates (r, θ, ϕ) (Fig. 2-3). Its transition dipole moment vector \mathbf{d}

lies tangent to the vesicle surface, in the $\theta\phi$ -plane. We define ω as the angle \mathbf{d} makes with $\hat{\theta}$ in the $\theta\phi$ -plane (Fig. 2-3a). We express \mathbf{d} in terms of its projections along $\hat{\theta}$ and $\hat{\phi}$, local unit vectors pointing in the direction of increasing θ and ϕ , respectively (Fig. 2-3a):

$$\mathbf{d} = d \cos \omega \hat{\theta} + d \sin \omega \hat{\phi} \quad (6)$$

We then expand $\hat{\theta}$ and $\hat{\phi}$ in terms of the original Cartesian (xyz) coordinate system:

$$\hat{\theta} = (\cos \theta \cos \phi) \hat{x} + (\cos \theta \sin \phi) \hat{y} - (\sin \theta) \hat{z} \quad (7)$$

$$\hat{\phi} = (-\sin \phi) \hat{x} + (\cos \phi) \hat{y} \quad (8)$$

which gives:

$$\mathbf{d} = (d \cos \omega \cos \theta \cos \phi - d \sin \omega \sin \phi) \hat{x} + (d \cos \omega \cos \theta \sin \phi + d \sin \omega \cos \phi) \hat{y} - (d \cos \omega \sin \theta) \hat{z} \quad (9).$$

The dot product of \mathbf{d} and \mathbf{E} is given by $\mathbf{E} \cdot \mathbf{d} = E d \cos \xi$, where ξ is the angle between these two vectors. For $E = d = 1$ and $\mathbf{E} = \hat{x}$,

$$\mathbf{E} \cdot \mathbf{d} = \cos \xi = \cos \omega \cos \theta \cos \phi - \sin \omega \sin \phi \quad (10).$$

The relative excitation efficiency is proportional to $\cos^2 \xi$ and we assume that ω uniformly samples all angles from 0 to 2π to obtain the relative excitation efficiency of donor j as:

$$W_{\text{exc}, D_j} = \int_0^{2\pi} (\cos \omega \cos \theta \cos \phi - \sin \omega \sin \phi)^2 d\omega \quad (11)$$

The FRET efficiency of a docked but unfused vesicle pair is then the weighted mean of the FRET efficiencies of all N_D donors:

$$E = \frac{\sum_{j=1}^{N_D} w_{\text{exc}, D_j} \cdot E_{D_j}}{\sum_{j=1}^{N_D} w_{\text{exc}, D_j}} \quad (12).$$

We used our best estimate for the Förster radius ($R_0 = 6$) to calculate the FRET efficiency E for pairs of docked but unfused vesicles labeled at 2%. The FRET efficiency depends on the orientation of the vesicles relative to \mathbf{E} (Fig. 2-3 *c, d*). In Fig. 2-3 *e* we present FRET efficiencies for modeled pairs of docked but unfused vesicles with donor radius R_D and acceptor radius R_A that sample many vesicle pair orientations. The vesicle pairs sample 11 different values of α in the range 0–90° (0, 9°...90°); for each α the pair samples 11 different values of β (0, 36°...360°). The average value of E at each α comes from equal weighting of the values obtained for each β .

The final orientationally averaged FRET efficiencies are presented in Fig. 2-3 *e*. These results average the E values obtained at each α with $\sin\alpha$ weighting to mimic a uniform distribution of orientations over a hemisphere. As shown, very small t-SNARE vesicles ($R_D = 15$ nm), which are rare, have FRET efficiencies in the range 0.12–0.22. Average-sized t-SNARE vesicles ($25 \text{ nm} < R_D < 50 \text{ nm}$) that are docked but unfused always have $E < 0.10$, and often much smaller. Large t-SNARE vesicles ($R_D > 50 \text{ nm}$) paired with any size acceptor vesicle always have $E < 0.05$. Our modeling shows that for the vast majority of docked but unfused vesicle pairs $E < 0.25$ and that exciting the donors with s-polarized light slightly enhances the mean FRET efficiency as compared with the case of donors that are uniformly excited (Fig. 2-3 *f*).

Determination of a FRET Efficiency Threshold

Next we calculate the probability that a vesicle *fusion* product would have $E < 0.25$ and potentially be confused with vesicle pairs in the docked but unfused state. Figure 2-2 shows that $E < 0.25$ occurs when a fused vesicle pair contains $< 0.2\%$ DiD. This would require that a t-SNARE vesicle dock and fuse with a v-SNARE vesicle with nine times less surface area. Assuming random pairing between our vesicles (Fig. 2-1), such a pairing would occur $< 2\%$ of the time. For the remaining $> 98\%$ of vesicle pairs full fusion will result a vesicle with $> 0.2\%$ DiD, and therefore $E > 0.3$. Modeling docked but unfused pairs suggests that for the vast majority of pairs $E < 0.25$ (Fig. 2-3). In summary, the modeling supports a cutoff of $E = 0.25$ and predicts a clean separation between populations of vesicles that are docked but unfused vs docked and fused. This threshold is supported by real time observation of single docking and fusion events (Fig. 3-6).

Calculated FRET Efficiencies for Docked and Hemifused Vesicle Pairs

For docked and hemifused vesicles, the hemifusion product was modeled as *two different pairs* of parallel planes with each pair spaced by 4 nm. One pair of planes models the hemifused donor vesicle while the other pair models the hemifused acceptor vesicle. The model of the hemifused donor vesicle has one plane containing 2% donor labels (to represent the unmixed donor inner leaflet) and one plane containing a mixture of donors and acceptors (to represent the mixed outer leaflet). The model of the hemifused acceptor vesicle has one plane containing 2% acceptor labels (to represent the unmixed acceptor inner leaflet) and one plane containing a

mixture of donors and acceptors (to represent the mixed outer leaflet). The labeling fractions of the mixed planes is the same for both vesicles, and is determined from the ratio of donor to acceptor vesicle surface areas. We assumed that there is no FRET between vesicles, so that we expect the model to slightly underestimate E for hemifusion.

In the hemifusion model, there are three different populations of donor labels that differ in the concentration of surrounding acceptors. Each donor population has its own donor quenching term ($S(t)$ in Eq. 1), and thus different average FRET efficiency E . For the donor vesicle inner leaflet, we set the minimum intra-plane spacing between labels to infinity ($a = \infty$, because there are no acceptors in the same plane as these donors) and the minimum inter-plane spacing as the thickness of the bilayer ($h = 4$ nm). In contrast, the donor labels present in the donor vesicle outer leaflet carry out FRET only to acceptors present in the same plane ($a = 0.84$ nm and $h = \infty$). The donor labels in a hemifused acceptor vesicle outer leaflet carry out FRET to acceptors in their own plane and in the other leaflet plane ($a = 0.84$ nm and $h = 4$ nm). For each docked and hemifused pair, the overall mean FRET efficiency E was calculated from the weighted average of the E values determined for the donors present in the three different leaflets. The results using $R_0 = 6$ nm are plotted in Fig. S8b; these can be directly compared with the results for full fusion in Fig. 2-4 a.

The model predicts a wide range of FRET efficiency values, $E = 0.25$ -1.0, arising from docked and fully fused vesicles when the donor and acceptor vesicles range in size from 15-75 nm (Fig. 2-2). Perhaps surprisingly, the model predicts a similar range of values, $E = 0.15$ -0.9, arising from docked and hemifused pairs. The two FRET efficiency distributions overlap severely. For given vesicle sizes in a vesicle pair, the difference in E between the hemifused and fused states varies only from 0.1 to 0.2. For example, two 45 nm vesicles that have docked and

hemifused have $E = 0.8$; once they fully fuse E increases only to 0.9. The difference between E for hemifusion vs full fusion is much smaller than the range of FRET efficiency values expected to arise from random pairing between vesicles with the size distribution used in this study.

Therefore, we conclude that we cannot distinguish between full fusion and hemifusion using the DiI/DiD FRET pair when the vesicles are originally labeled at 2%.

2.4) Discussion

The strategy of this single-vesicle assay is to label v-SNARE vesicles with red-fluorescent lipid labels and t-SNARE vesicles with green-fluorescent lipid labels and use the extent of Förster resonance energy transfer (FRET) from the green labels to the red labels to distinguish between docked but unfused t-SNARE/v-SNARE vesicle pairs from docked and fused pairs (Yoon et al., 2006). We performed quantitative modeling and found that for >98% of the v- and t-SNARE vesicle pairs the FRET efficiency from green to red labels will accurately distinguish docked but unfused from docked and fused states using our labeling scheme. The modeling shows that we cannot distinguish between full fusion and hemifusion states.

Imaging single vesicle in this docking and fusion assay requires one set of vesicles to be immobilized to a surface for imaging with total internal reflection microscopy (TIRFM). To achieve vesicle immobilization we used a novel tethering system which conjugated the v-SNARE vesicles to a PEG polymer cushion that was in turn anchored to a lipid bilayer on glass. The tethered vesicles diffuse, proving that tethered vesicles do not make contact with the underlying glass support. Previous work from our lab showed that the lipids and proteins present in a ruptured giant unilamellar vesicle enjoy free homogenous diffusion when they are tethered to this PEG-bilayer surface, which provides strong support that the diffusion of the lipids and proteins in our tethered vesicles is also unhindered (Wang et al., 2010).

2.5) Experimental Procedures

Preparation of Proteoliposomes

Recombinant neuronal SNARE proteins were expressed and purified from bacteria. A detailed description of the plasmids, cell lines, buffers, and procedures used has been given previously (Tucker et al., 2004). The specific proteins used were the full-length, wild type v-SNARE protein mouse synaptobrevin-2 His₆ (syb) and rat His₆ syntaxin-1A (syx); a binary t-SNARE complex composed of syx and mouse His₆ SNAP-25B; and a binary t-SNARE complex composed of syx and a truncated version of mouse His₆ SNAP-25B (syx + SNAP-25Δ26), which was designed to correspond to the SNAP-25 fragment that would be left following cleavage with *Clostridium botulism* neurotoxin serotype E (BoNT/E) (Tucker et al., 2004). Both t-SNARE heterodimers were co-expressed from a dicistronic vector in bacteria, then purified and reconstituted simultaneously into vesicles.

The t-SNARE and v-SNARE proteins were reconstituted by the co-micellization method into proteoliposomes, as described in detail previously (Axelrod, 2001). The lipid content is 55% (mol/mol) 1-palmitoyl, 2-oleoyl phosphatidylcholine (POPC), 15% 1,2-dioleoyl phosphatidylserine (DOPS) and 28% 1,2-dioleoyl phosphatidylethanolamine (DOPE). The v-SNARE vesicles are labeled with 2% 1,1'-dioctadecyl-3,3,3',3'-tetramethylindodicarbocyanine, 4-chlorobenzenesulfonate (DiD) and 0.2% 1,2-dipalmitoyl-*sn*-glycero-3-phosphoethanolamine-N-(biotinyl) (biotin PE); t-SNARE vesicles are labeled with 2% 1,1'-dioctadecyl-3,3,3',3'-tetramethylindodicarbocyanine perchlorate (DiI). All synthetic phospholipids were purchased from

Avanti Polar Lipids (Alabaster, AL). Fluorescent labels were purchased from Molecular Probes (Eugene, OR).

Proteoliposomes were purified away from unincorporated lipids, detergent, and proteins by flotation in an Accudenz (Accurate Chemical, Westbury, NY) step gradient. Protein incorporation was confirmed by sodium dodecyl sulfate polyacrylamide gel electrophoresis (SDS-PAGE). To remove Accudenz from the fusion experiments, purified t-SNARE vesicles were put into dialysis membranes (Spectra/Por 6-8,000 molecular weight cutoff, Spectrum Laboratories, Inc. Rancho Dominguez, CA) and dialyzed overnight against 25 mM HEPES·KOH, 100 mM KCl, 10% glycerol, and 1 mM dithiothreitol (pH 7.40) (all salts from Sigma-Aldrich) at 4 °C. Assuming similar protein and lipid recovery as measured directly by Tucker et al. (Tucker et al., 2004), purified donor vesicles have ~95 total t-SNARE/syx + SNAP-25Δ26/ syx (~65 “correctly oriented”) copies per vesicle and were harvested at 2.7 mM lipid (assuming the average vesicle contains 27,000 lipids, this corresponds to 100 nM vesicles). Acceptor vesicles have ~60 syb (~45 “correctly oriented”) copies per vesicle on average. It is possible that the protein copy number is highly variable from vesicle to vesicle (Chen et al., 2006). The vesicles were used fresh or flash-frozen in liquid Nitrogen and stored at -80 °C.

Tethering of v-SNARE vesicles to a PEG-Functionalized Supported Lipid Bilayer

To form the passivating layer, protein-free liposomes composed of 80% POPC, 15% DOPS, and either 5% 1,2-distearoyl-*sn*-glycero-3-phosphoethanolamine-N-[methoxy(polyethylene glycol)-2000] (PEG) or 5% 1,2-distearoyl-*sn*-glycero-3-phosphoethanolamine-N-[biotinyl(polyethylene glycol)-2000] (Biotin-PEG) were prepared using

the same reconstitution and purification procedure as used for the SNARE-bearing vesicles. Purified vesicles were introduced above a clean, hydrophilic glass coverslip (Fisherfinest Premium Cover Glasses, Fisher Scientific, Waltham, MA) where they spontaneously formed a supported lipid bilayer (SLB).

Supported lipid bilayers for use in the tethered vesicle fusion experiments were nearly free of defects that cause non-specific binding of v-SNARE and t-SNARE vesicles. Typically, the bilayers used for these experiments had <5 defects per $6400\ \mu\text{m}^2$ of surface area, as was assayed frequently by introducing a dilute solution of vesicles above the bilayer. Bilayers of sufficient quality were achieved by depositing the vesicles at a low temperature using a protocol developed previously in our lab (Liu et al., 2005). A 4:1 mixture of PEG: biotin-PEG vesicles were diluted a factor of 100 ($\sim 30\ \mu\text{M}$ total lipid) in Membrane-Making Buffer (MMB; 25 mM HEPES·KOH and 100 mM KCl, pH 7.40). Fresh MMB was made frequently and filtered using $0.22\ \mu\text{m}$ pore cellulose acetate membranes (Corning Life Sciences, Lowell, MA). The vesicles were deposited into the sample cells at room temperature, stored in a covered glass dish, and immediately placed into a 4°C refrigerator. After ≥ 2.5 hr, the glass dish was moved to a 37°C incubator (Model 1525, VWR International, West Chester, PA) for ≥ 4 hr. The bilayers could be stored at 4°C overnight or in the 37°C incubator for up to ~ 5 hr, provided they did not dry out. A clean glass coverslip served as the bottom face and “window” into our homemade sample cell. Coverslips were cleaned by sonication in a $\sim 20\%$ v/v detergent solution (Contrad-70, Decon Labs Inc, **King of Prussia, PA**), rinsed extensively using $18.2\ \text{M}\Omega\cdot\text{cm}$ Millipore water (Millipore Simplicity system, Billerica, MA), etched for 1 hour at 90°C by incubation in a commercial mixture of sulfuric acid and hydrogen peroxide (Nanostrip, Cyantek, Billerica, MA), and then again rinsed extensively with Millipore water before use.

Unfused PEG/Biotin-PEG vesicles were rinsed away from supported lipid bilayers by flushing each sample cell with 2 mL of 37°C MMB while the sample cells were kept at 37°C within a modified benchtop drybath. To tether the v-SNARE vesicles, a 0.2 mg/mL solution of NeutrAvidin biotin-binding protein (ImmunoPure, Pierce, Rockford, IL) in MMB was incubated with the bilayer for 3 min then rinsed away with 3 mL of MMB. An optimal density of ~200 tethered vesicles per 3000 μm^2 surface area was achieved by first diluting the purified v-SNARE vesicles 25 times in MMB and then incubating the vesicle solution with the NeutrAvidin-functionalized surface for 20 min. After 20 min, excess v-SNARE vesicles were rinsed away using 2 mL MMB. The number of t-SNARE vesicles that non-specifically bind to the surface increased a factor of ~10-100 after functionalization with NeutrAvidin.

2.6) Figures

Figure 2-1

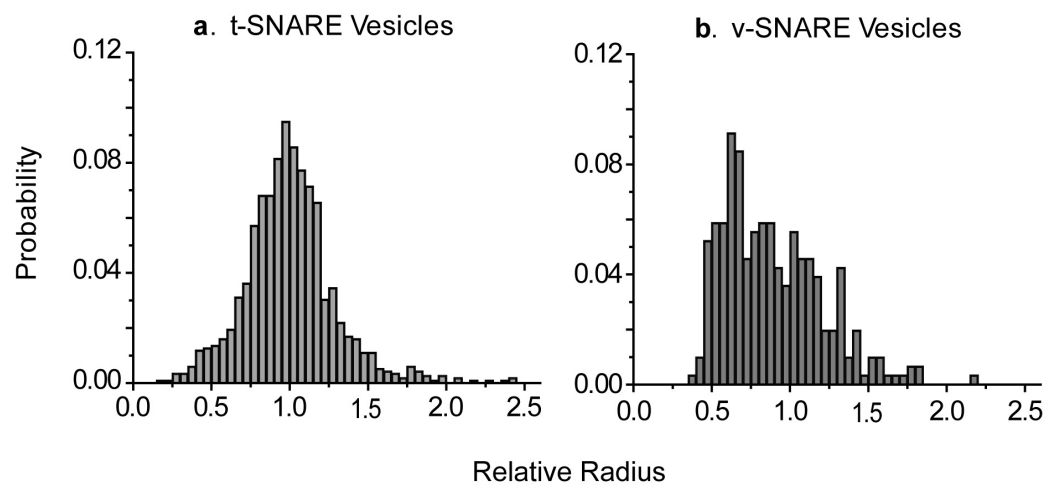


Figure 2-1. Relative Size Distribution of v-SNARE and t-SNARE Vesicles

The relative radius of each vesicle was determined from the square-root of its background-corrected fluorescence intensity. Histograms show the relative radii of the entire population of *a*) DiI-labeled t-SNARE vesicles and *b*) DiD-labeled v-SNARE vesicles. The two histograms were placed on the same relative scale after correcting for differences in excitation and emission efficiencies of the labels. Electron microscopy of similarly prepared vesicles found that the t- and v-SNARE vesicles have a mean radius of 33 nm and 39 nm, respectively, and that both v- and t-SNARE vesicle radii range from 15-75 nm. (Personal communication from Enfu Hui and Ed Chapman, UW-Madison Dept. of Physiology).

Figure 2-2

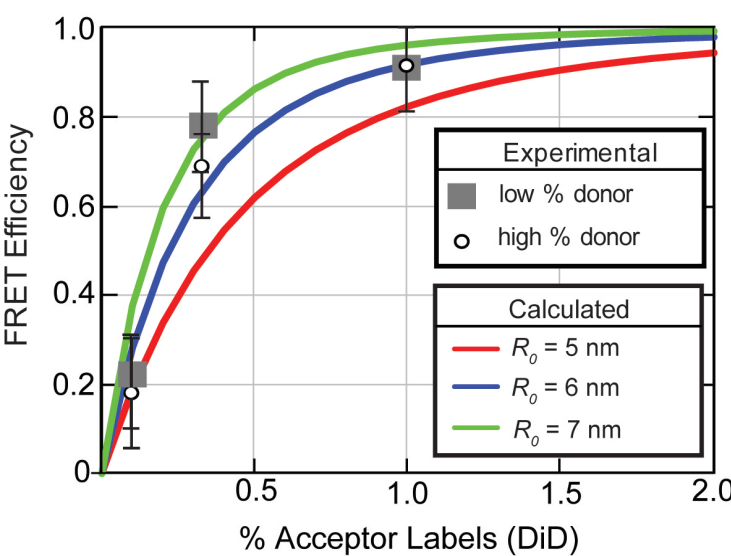
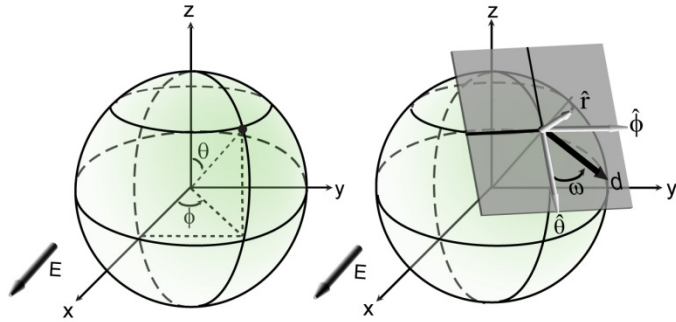


Figure 2-2. FRET Efficiencies of Mixed Vesicles

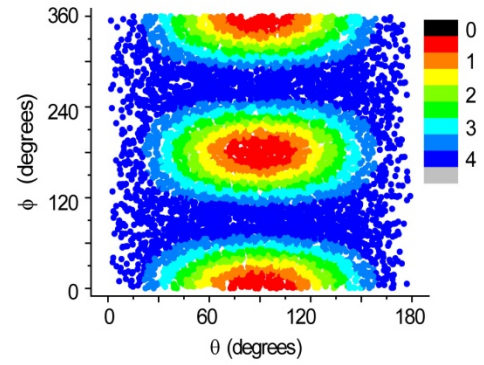
To simulate full fusion between different-sized v-SNARE and t-SNARE vesicles, mixed-label vesicles were reconstituted with varying fraction of DiI (donor) and DiD (acceptor) labels. The mixed vesicles were immobilized on glass and the FRET efficiency from DiI to DiD was measured (Eq. 16). Three different acceptor fractions were used, each at two different donor fractions. Specifically, the “high % donor” mixtures (open circles) were: 0.1% DiD + 1.9% DiI, 0.33% DiD + 1.67% DiI, and 1% DiD + 1% DiI. The “low % donor” mixtures (gray squares) were: 0.1% DiD + 0.48% DiI, 0.33% DiD + 0.42% DiI, and 1% DiD + 0.25% DiI. Smooth curves are the calculated FRET efficiency vs % Acceptor labels for our model of fully fused vesicles. The model calculates FRET efficiency for a randomly distributed mixture of donor and acceptor labels lying in two parallel planes spaced by 4 nm. Three different Förster radii were tested: $R_0 = 5$ nm (red line), 6 nm (blue line), and 7 nm (green line).

Figure 2-3.

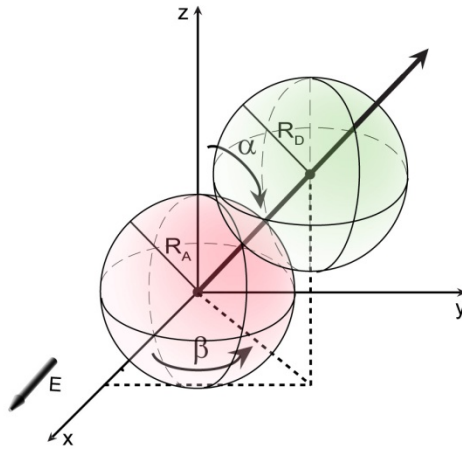
a. Coordinate Systems Define Donor Position and Transition Dipole Orientation



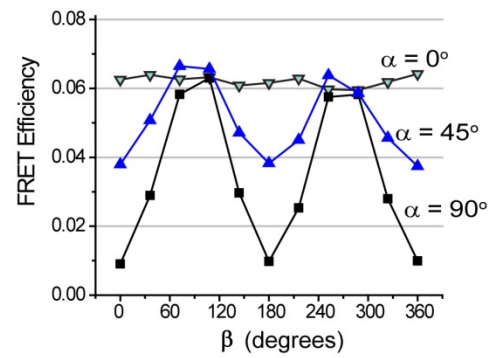
b. Relative Excitation Efficiencies of Donors



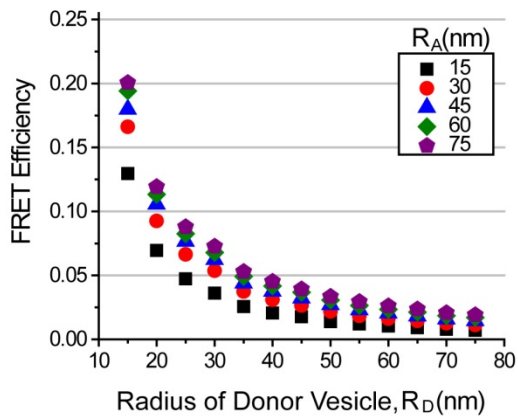
c. Docked but Unfused Vesicles' Orientation



d. Orientation Effects on FRET Efficiency ($R_D = R_A = 35$ nm)



e. FRET Efficiencies of Docked but Unfused Pairs that Sample Many Vesicle Orientations



f. FRET Efficiencies of Docked but Unfused Pairs Assuming Uniform Donor Excitation

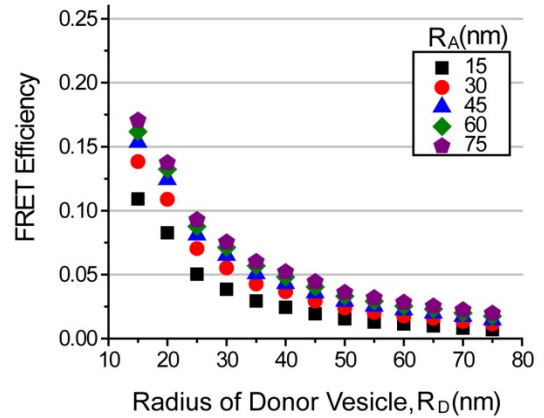
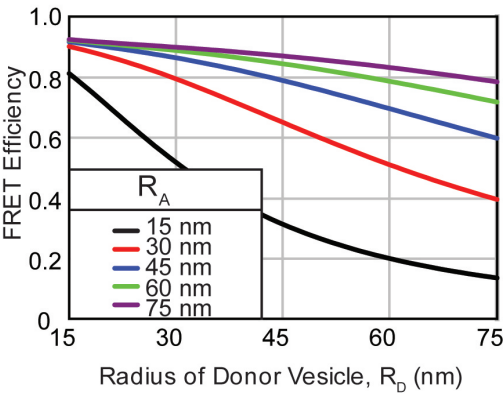


Figure 2-3. Model Estimates of FRET Efficiency for Docked but Unfused Vesicle Pairs

Docked but unfused vesicle pairs are modeled as a pair of touching spheres. Each sphere has two surfaces (lipid bilayer leaflets) that are separated by 4 nm and decorated with a random distribution of labels. The donor labels are excited with an s-polarized evanescent wave whose electric-field vector \mathbf{E} points in the x-direction in the Cartesian (xyz) coordinate system; the glass coverslip in the experiment lies in the xy-plane. *a)* The position of a donor label on the surface of the sphere is specified in spherical polar coordinates by its polar angle θ and azimuthal angle ϕ . Originating from its position are three local, mutually orthogonal unit vectors $\hat{\mathbf{r}}$, $\hat{\boldsymbol{\theta}}$, and $\hat{\boldsymbol{\phi}}$ that point in the direction of increasing r , θ , and ϕ , respectively. The donor transition dipole moment vector \mathbf{d} lies tangent to the surface of the sphere. Its projections along $\hat{\boldsymbol{\theta}}$ and $\hat{\boldsymbol{\phi}}$ are determined by the angle between \mathbf{d} and $\hat{\boldsymbol{\theta}}$, which we call ω . In the FRET calculations, ω is assumed to be uniformly distributed in the $\theta\phi$ -plane. *b)* Color map indicating donor relative excitation efficiencies according to the (θ, ϕ) location on the sphere. Labels whose transition dipoles on average lie more nearly parallel to the electric vector \mathbf{E} (at the vesicle “poles”, for example) are excited more efficiently than those that lie on average more perpendicular to \mathbf{E} . *c)* The orientation of a docked but unfused vesicle pair is defined by a vector that connects the two vesicle centers. The orientation of this vector is specified a polar angle α and azimuthal angle β . *d)* Calculated FRET efficiency for a model pair of 35-nm radius vesicles that are docked but unfused using $R_0 = 6$ nm. FRET efficiency is plotted vs β for the values $\alpha = 0^\circ, 45^\circ, 90^\circ$. *e)* The mean FRET efficiency for a docked but unfused vesicle pair with donor radius R_D and acceptor radius R_A that samples different values of α and β . Effects of laser polarization on excitation efficiency are included. *f)* Same as in panel *e*, except that all donors are excited with equal efficiency (no polarization effects).

Figure 2-4

b. Docked and Hemifused



a. Docked and Fully Fused

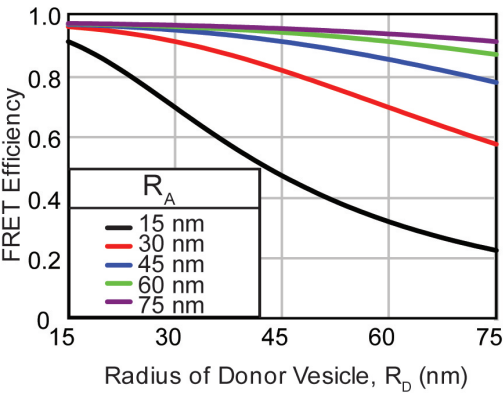


Figure 2-4. Model Estimates of Docked and Fused FRET Efficiency E

a) Docked and fully fused vesicles were modeled as one pair of parallel planes (“lipid bilayer leaflets”) that each contains a random distribution of donor and acceptor labels. The FRET efficiency E depends on the final acceptor labeling fraction and the Förster radius. We fixed the final acceptor concentration from the ratio of donor to acceptor vesicle surface areas (assuming spherical geometries). Plotted is E vs donor vesicle radius for a number of different acceptor radii using $R_0 = 6$ nm. *b)* Docked and hemifused vesicles were modeled as two separate pairs of parallel planes (no inter-vesicle FRET). The hemifused donor “vesicle” is modeled as one plane containing 2% donor labels and one mixed plane (containing both donors and acceptors). The hemifused acceptor “vesicle” is modeled as one plane containing 2% acceptor labels and one mixed plane. The labeling fractions of the mixed plane were the same for both vesicles and determined from the ratio of the outer leaflet surface areas of the vesicle pair. The FRET efficiency was calculated for each plane using $R_0 = 6$ nm. Plotted is the weighted average of FRET efficiency for each plane, with the weights reflecting the relative concentration of donor labels.

Figure 2-5

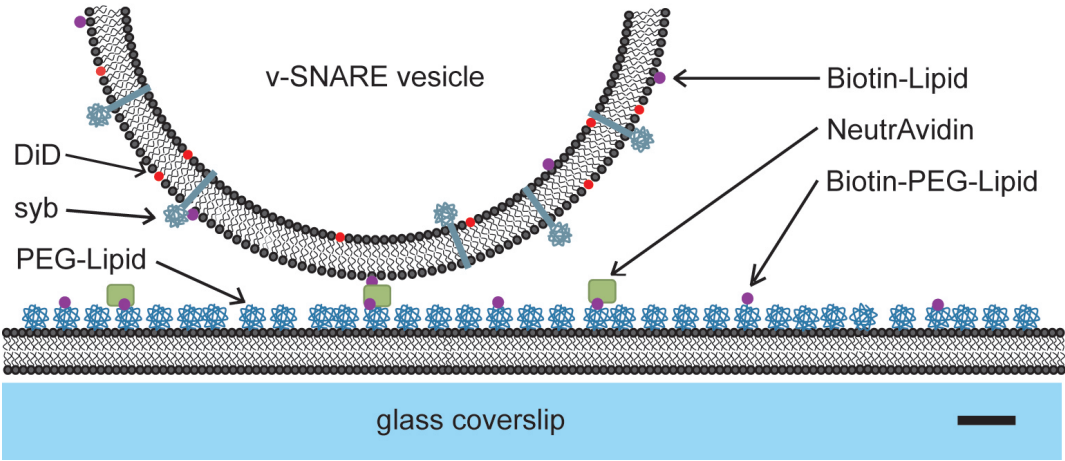


Figure 2-5. Schematic of Vesicle Tethering Method

The v-SNARE vesicles are tethered via biotin-NeutrAvidin interactions to a PEG-functionalized lipid bilayer supported on glass. The v-SNARE vesicle membrane contains 0.2% biotin-PE and the supported lipid bilayer contains 1% biotin-PEG-DPPE. Scale bar = 5 nm.